Journal of Oceanology and Limnology
Vol. 39 No. 4, P. 1328-1342, 2021
https://doi.org/10.1007/s00343-020-0234-z

Carbon biomass, carbon-to-chlorophyll *a* ratio and the growth rate of phytoplankton in Jiaozhou Bay, China*

Shujin GUO[1, 2, 3], Zengxia ZHAO[1, 2, 3], Junhua LIANG[1, 2, 3], Juan DU[1, 2, 3], Xiaoxia SUN[1, 2, 3, 4, **]

[1] *Jiaozhou Bay National Marine Ecosystem Research Station*, *Chinese Academy of Sciences*, *Qingdao 266071*, *China*

[2] *Laboratory for Marine Ecology and Environmental Science*, *Pilot National Laboratory for Marine Science and Technology* (*Qingdao*), *Qingdao 266237*, *China*

[3] *Center for Ocean Mega-Science*, *Chinese Academy of Sciences*, *Qingdao 266071*, *China*

[4] *University of Chinese Academy of Sciences*, *Beijing 100049*, *China*

Received Jun. 17, 2020; accepted in principle Jul. 29, 2020; accepted for publication Oct. 15, 2020

Abstract Carbon biomass, carbon-to-chlorophyll *a* ratio (C:Chl *a*), and the growth rate of phytoplankton cells were studied during four seasonal cruises in 2017 and 2018 in Jiaozhou Bay, China. Water samples were collected from 12 stations, and phytoplankton carbon biomass (phyto-C) was estimated from microscope-measured cell volumes. The phyto-C ranged from 5.05 to 78.52 μg C/L in the bay, and it constituted a mean of 38.16% of the total particulate organic carbon in the bay. High phyto-C values appeared mostly in the northern or northeastern bay. Diatom carbon was predominant during all four cruises. Dinoflagellate carbon contributed much less (<30%) to the total phyto-C, and high values appeared often in the outer bay. The C:Chl *a* of phytoplankton cells varied from 11.50 to 61.45 (mean 31.66), and high values appeared in the outer bay during all four seasons. The phyto-C was also used to calculate the intrinsic growth rates of phytoplankton cells in the bay, and phytoplankton growth rates ranged from 0.56 to 1.96/d; the rate was highest in summer (mean 1.79/d), followed by that in fall (mean 1.24/d) and spring (mean 1.17/d), and the rate was lowest in winter (mean 0.77/d). Temperature and silicate concentration were found to be the determining factors of phytoplankton growth rates in the bay. To our knowledge, this study is the first report on phytoplankton carbon biomass and C:Chl *a* based on water samples in Jiaozhou Bay, and it will provide useful information for studies on carbon-based food web calculations and carbon-based ecosystem models in the bay.

Keyword: phytoplankton; carbon biomass; carbon-to-chlorophyll *a* (C:Chl *a*) ratio; growth rates; Jiaozhou Bay

1 INTRODUCTION

Phytoplankton biomass is strongly related to food web structure, which influences the energy flow and material cycling in the ocean (Friedland et al., 2012). Therefore, determining the phytoplankton biomass is important for understanding the food web structures in the oceans (Arteaga et al., 2016). Determination of cell abundance of phytoplankton by direct counting the number of cells is often used to determine the phytoplankton biomass. However, as different phytoplankton species have different shapes and sizes, phytoplankton biomass by the counting would underestimate the contribution of large species while overestimate the contribution of small species (Harrison et al., 2015). Chlorophyll *a* (Chl *a*) or ATP could also be used to express phytoplankton biomass, but they can only provide information on the whole phytoplankton group (Gong et al., 1996; Kruskopf and Flynn, 2006). Therefore, a standard biomass estimate is essential for estimating phytoplankton biomass with various phytoplankton species in natural samples (Arteaga et al., 2016).

* Supported by the National Natural Science Foundation of China (Nos. 31700425, 91751202), the External Cooperation Program of Chinese Academy of Sciences (No. 133137KYSB20200002), and the Taishan Scholars Project to Song SUN
** Corresponding author: xsun@qdio.ac.cn

In studying marine ecosystems, it is usually desirable to express phytoplankton biomass as organic carbon, which will facilitate a quantitative assessment of the relationship between different marine food web levels (Graff et al., 2015). Furthermore, expressing phytoplankton biomass in carbon (phyto-C) is the only way to represent phytoplankton biomass in a biogeochemical model that includes nonliving carbon contents (Arteaga et al., 2016). Phyto-C could also be used to calculate the growth rate of the whole phytoplankton community based on primary productivity measurements (Regaudie-de-Gioux et al., 2015), which is important to understand many oceanographic processes, such as the vertical flux of organic matter, nutrient utilization patterns and yield from the food web (Smith et al., 1999). Therefore, phyto-C is a quite useful parameter to express phytoplankton biomass in the ocean. To our knowledge, no method has existed for directly measuring phyto-C in natural populations, which has mainly been due to an inability to separate phytoplankton cells from other constituents contributing to the total particulate organic carbon (POC) pool (e.g., zooplankton, heterotrophic bacteria, and detritus), and a carbon-to-chlorophyll *a* ratio (C∶Chl *a*) is usually used to convert measured Chl *a* to phyto-C in marine ecosystems (Arteaga et al., 2016). However, the relationship between Chl *a* and phyto-C is not constant, and a wide range of C∶Chl *a* values (from 6 to 333) have been reported across laboratory and field studies (Cloern et al., 1995; Sathyendranath et al., 2009). To date, the 'gold standard' of estimating phyto-C has been to measure the dimensions of phytoplankton cells, calculate their volume, and then convert that volume to carbon biomass using the volume-to-carbon conversion factor (Menden-Deuer and Lessard, 2000; Harrison et al., 2015). This approach is the only way to estimate phyto-C biomass at the species level, and it has been widely used in recent years (Jakobsen and Markager, 2016; Yang et al., 2017; Crawford et al., 2018).

Coastal seas are highly productive environments for aquatic organisms, attributable to greater phytoplankton biomass and primary production rates due to high nutrients concentrations than found in offshore oceanic areas (Chang et al., 2003b). The phytoplankton biomass and their growth rates are strongly related to food web structure, which influences energy flow and carbon cycles in marine ecosystems (Ara et al., 2019). Therefore, studying phytoplankton biomass and their growth rates is essential to understand the food web structure and biological productivity of the coastal environments, and is significant in evaluating the role of phytoplankton in carbon cycles in these areas. Seasonal variations in phytoplankton biomass have been extensively studied in temperate coastal seas in China (e.g. Fu et al., 2009; Zhou et al., 2012; Guo et al., 2014; Liu et al., 2015). However, almost all of these studies were based on the determination of phytoplankton cell abundance or Chl *a*, with studies on phytoplankton carbon biomass being limited. Until now, only limited studies have been carried out on phytoplankton carbon biomass in temperate coastal seas in China. Sun et al. (2000) compared different methods for calculating phytoplankton carbon in China Sea. Chang et al. (2003b) studied spatial variations of the C∶Chl *a* of phytoplankton in the East China Sea during a cruise in summer, 1998. Yang et al. (2017) estimated the carbon biomass of marine net phytoplankton from abundance in the Yellow Sea and East China Sea. Most of these studies were based on field investigations conducted only once in a season, or use net samples which would lose small phytoplankton cells. To our knowledge, there has been none study on spatio-temporal variation of phytoplankton carbon biomass in coastal China Seas based on water collecting samples, which would not be beneficial for our comprehensive understanding on the marine ecosystem.

As a semi-enclosed bay, Jiaozhou Bay is located on the northeastern coast of China and is adjacent to the South Yellow Sea. It covers an area of approximately 400 km^2, and the average depth is 7 m. Several small rivers with varying water loads empty into the bay (Guo et al., 2019). Due to its ecological and economic importance, Jiaozhou Bay has been chosen as a long-term ecosystem study area for temperate coastal seas in China by the Chinese Ecosystem Research Network since 1991. To date, there have been many studies on phytoplankton biomass and community structure in the bay (e.g., Sun et al., 1999, 2011a; Liu et al., 2002; Wu et al., 2005; Sun and Sun, 2012; Guo et al., 2019), which provide valuable information on phytoplankton ecology in this area. However, almost all of these studies were based on the determination of phytoplankton cell abundance or Chl *a*, and few determined phytoplankton biomass in terms of carbon (Sun et al., 2000; Lü et al., 2009), providing little information for the biogeochemical cycle (especially carbon cycle) and ecological dynamic model in this area. In this study, we determined phyto-C using

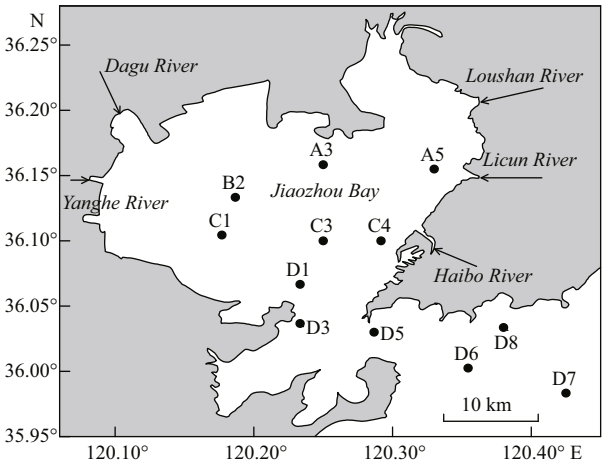

Fig.1 Study area and sampling stations in the Jiaozhou Bay

geometric models (Hillebrand et al., 1999; Sun and Liu, 2003) in Jiaozhou Bay and elucidated its spatial variations and regulators. As a conversion factor to estimate carbon biomass, the C∶Chl *a* of phytoplankton was also analyzed to provide a reference for subsequent studies on phytoplankton biomass in the bay. Finally, as an application, phyto-C was combined with ^{14}C-measured primary productivity to calculate phytoplankton growth rates in the bay. This study should provide useful information for the phytoplankton ecology and biogeochemical cycle (carbon cycle) in Jiaozhou Bay.

2 METHOD

2.1 Study area and sampling stations

Four seasonal cruises were carried out in Jiaozhou Bay in summer (August 17–18) and fall (November 9–10) 2017, and winter (February 1–2) and spring (May 9–10) 2018. Twelve stations were sampled during each cruise in the bay (Fig.1). Station D3, D5, D6, D8 and D7 were located in the outer bay, and other stations were in the inner bay.

2.2 Sampling and analysis

Temperature and salinity were determined with YSI 6600 Sonde (Yellow Springs, Ohio) at each station. Water transparency was measured with Secchi disk. Water samples were collected from the 0.5-m layer, and nutrients, Chl *a*, POC, phytoplankton composition, abundance, and cell volume were determined.

Nutrients, including nitrate (NO_3^-), nitrite (NO_2^-), ammonium (NH_4^+), phosphate (PO_4^{3-}) and silicate (SiO_3^{2-}), were determined using an autoanalyzer (model, SkalarSAN^{plus}, Skalar Analysis, the Netherlands) according to the method described in Guo et al. (2019). Chl *a* was filtered through GF/F filters (25 mm, Whatman^{TM}) and stored at -20 °C in the dark. In the laboratory, Chl *a* was extracted with 90% acetone at -20 °C for 24 h in the dark and then measured using a Turner-Designs Trilogy^{TM} laboratory fluorometer. POC was measured by filtering 300-mL seawater through precombusted GF/F filters (0.7 μm pore size, 1 h, 550 °C) under low vacuum (<1.33×10^4 Pa). The filters were then frozen at -20 °C. To remove inorganic matter, the filters were exposed to the HCl-saturated atmosphere for 24 h and then dried and analyzed with a CHN autoanalyzer (Perkin-Elmer 240) (Guo et al., 2019).

Phytoplankton samples were fixed in acidic Lugols (2% final concentration). In the laboratory, phytoplankton cells were concentrated with 25-mL settlement chambers for 24–48 h, and then identified and counted with an inverted microscope (Utermöhl, 1958). The cell volume of each species was calculated from measured dimensions by assigning an appropriate geometrical shape (Hillebrand et al., 1999; Sun and Liu, 2003). For the dominant phytoplankton species, at least 30 cells were measured. For the non-dominant phytoplankton species, 10–15 cells were measured. The measured dimensions were averaged and used to calculate the cell volume of phytoplankton species. The volume of the individual cells was then converted to carbon biomass with the volume-to-carbon conversion according to equation1.

$$C_c = a \times V_c^b, \tag{1}$$

where C_c is cell carbon, V_c is cell volume, *a* and *b* are 0.288 and 0.811 for diatoms, and 0.216 and 0.939 for dinoflagellates and other phytoplankton groups, respectively (Menden-Deuer and Lessard, 2000). The total phyto-C at each station was obtained by summing the carbon biomass of each species at each station.

Primary productivity was measured at 3 stations (A5, C3, and D7) by the ^{14}C assimilation method as described in Sun et al. (2011b). The phytoplankton growth rates (μ) at these stations were then estimated based on Eq.2 (Cloern et al., 1995; Chang et al., 2003b):

$$\mu = 0.85 \times P^B \left(\frac{\text{Chl } a}{C_p} \right) - 0.015, \tag{2}$$

where P^B is the chlorophyll-specific primary productivity, and C_p is the phyto-C.

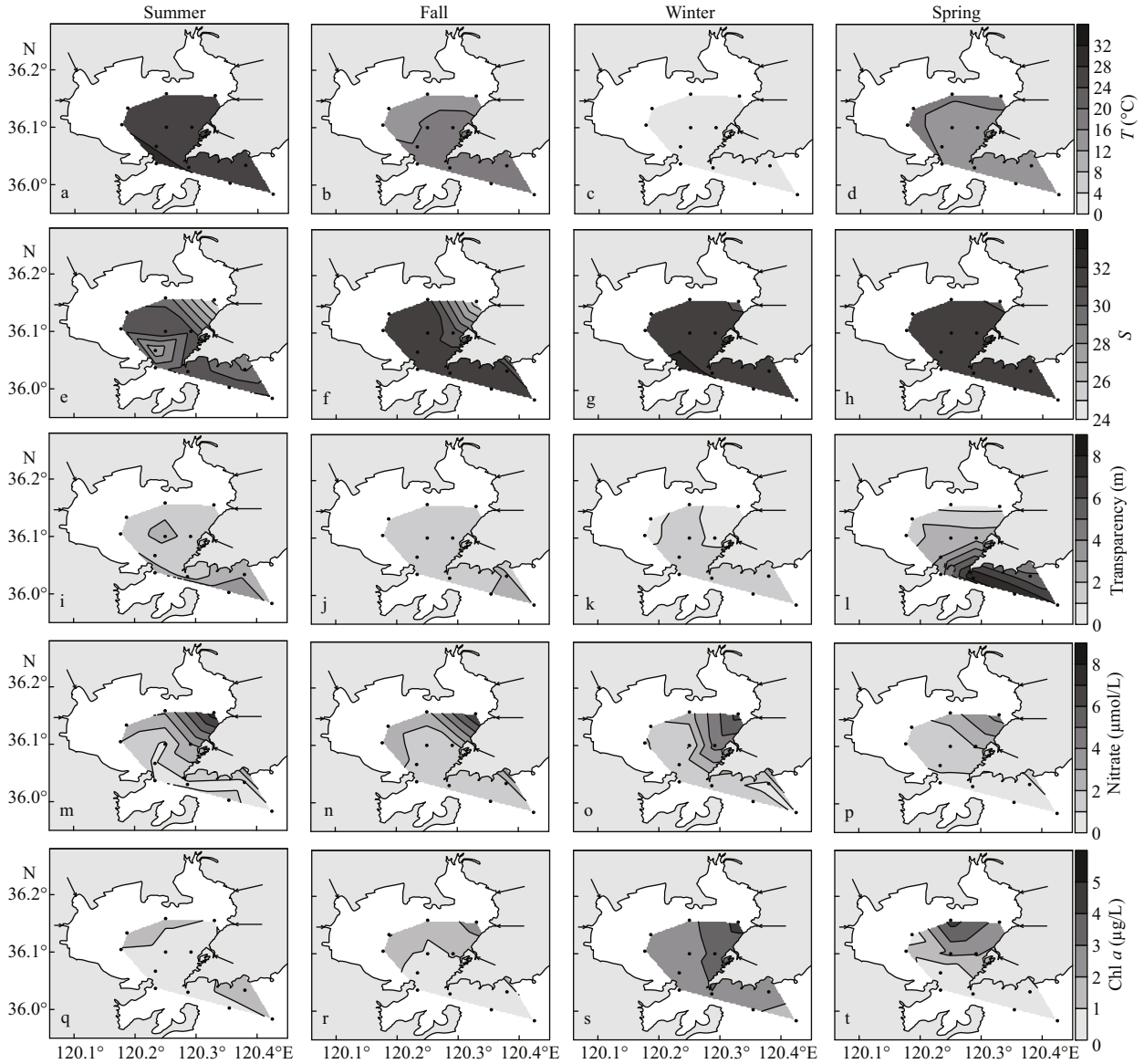

Fig.2 Distributions of surface temperature (*T*, ℃) (a–d), salinity (*S*) (e–h), transparency (m) (i–l), nitrate (μmol/L) (m–p), and Chl *a* (μg/L) (q–t) in the study area during four cruises

2.3 Data analysis

The dominance index (Y) of phytoplankton species is calculated based on Eq.3:

$$Y=\frac{n_i}{N}\times f_i, \tag{3}$$

where n_i is the sum of species i cell abundance; N is the sum of all species cell abundance values; and f_i is the species i occurrence frequency in all the samples.

Pearson correlation analysis (PCA) was carried out between the phytoplankton carbon biomass and environmental parameters. Canonical correspondence analysis (CCA) was used to examine the relationships between the environmental variables and dominant species. Students' t-test was used to made statistical comparisons, and $P<0.05$ was considered to represent a statistically significant difference.

3 RESULT

3.1 Hydrographic conditions

Surface temperature, salinity, transparency, nitrate, and Chl-*a* concentration in the bay during the four cruises are presented in Fig.2. High surface temperature value appeared in the outer bay during summer, fall, and winter (Fig.2a–c). In spring, high temperature value appeared in the northern part of the study area (Fig.2d). Of the stations, station A5 had the lowest surface salinity during all four cruises (Fig.2e–h). High values of transparency were always

Table 1 Means of environmental parameters at each cruise in the Jiaozhou Bay

Season variable	Summer average (±SD)	Fall average (±SD)	Winter average (±SD)	Spring average (±SD)
Temperature (°C)	27.35±1.14	16.38±1.30	2.45±1.54	15.03±1.52
Salinity	29.56±1.83	30.99±1.74	31.76±0.34	31.70±0.31
Transparency (m)	2.03±0.91	1.53±0.41	1.39±0.56	3.71±2.59
SiO_3^{2-} (μmol/L)	4.50±3.56	2.03±0.60	0.85±0.78	1.42±1.51
PO_4^{3-} (μmol/L)	0.18±0.18	0.15±0.09	0.09±0.05	0.10±0.09
NO_3^- (μmol/L)	2.04±1.91	1.53±1.06	1.40±1.09	1.38±1.16
Chl *a* (μg/L)	0.92±0.43	1.07±0.59	2.64±0.69	1.19±1.33
Phyto-C (μg C/L)	35.41±11.93	16.27±6.90	41.93±17.99	21.57±16.90
Diatom-C (μg C/L)	30.32±15.96	15.44±7.54	40.97±18.18	19.05±18.66
Dinoflagellate-C (μg C/L)	5.09±7.71	0.73±1.03	0.95±1.03	2.41±3.92

SD: standard deviation.

observed in the outer bay during the four cruises (Fig.2i–l). The nitrate concentration showed a similar distribution pattern with salinity, and it was higher in the inner bay than in the outer bay (*t*-test, $P<0.05$) (Fig.2m–p). The Chl-*a* concentration varied from 0.05 to 4.43 μg/L in the study area, and its distribution pattern was consistent with that of nitrate, except in summer, when a high value appeared at station D7 (Fig.2q–t). The means of the environmental parameters during each cruise are presented in Table 1. Temperature was highest in summer, followed by that in fall and spring, and it was lowest in winter. Salinity was lowest in summer, and the mean values were similar among the four cruises. The mean transparency was higher in summer and spring than in fall and winter. For the nutrients, the concentrations of SiO_3^{2-}, PO_4^{3-}, and NO_3^- were highest in summer, followed by those in fall, and they were the lowest in winter and spring.

3.2 Carbon biomass of phytoplankton cells

Phyto-C in the study area ranged from 16.07 to 62.76 μg C/L (mean 35.41 μg C/L) in summer, 7.77 to 32.04 μg C/L (mean 16.27 μg C/L) in fall, 24.45 to 78.52 μg C/L (mean 41.93 μg C/L) in winter and 5.05 to 60.52 μg C/L (mean 21.57 μg C/L) in spring (Table 1). High values of phyto-C were always observed in the northern or northeastern bay (Fig.3a–d). Diatom carbon biomass (diatom-C) was predominant in the bay, at mean values of 83%, 91%, 93%, and 76% of the total phyto-C during four cruises, respectively. The distribution pattern of diatom-C was similar to that of phyto-C. Dinoflagellate carbon biomass (dinoflagellate-C) was quite low, and the mean value was higher in spring (mean 19.05 μg C/L) and summer (mean 5.09 μg C/L) than in fall (mean 0.73 μg C/L) and winter (mean 0.95 μg C/L). The distribution pattern of dinoflagellate-C was different from diatom-C, and high values always appeared in the southern part of the study area (Fig.3i–l).

Phyto-C/POC ranged from 22.89% to 56.65% (mean±SD=39.82%±10.34%) in summer, 21.99% to 32.19% (mean±SD=26.39%±3.23%) in fall, 25.33% to 62.89% (mean±SD=47.20%±10.68%) in winter and 17.47% to 66.36% (mean±SD=39.25%±15.42%) in spring. For the whole year, phyto-C/POC ranged from 17.47% to 66.36% (mean±SD=38.16%±13.17%) in the study area.

The relationships between phytoplankton carbon biomass and the environmental parameters in the bay are shown in Table 2. Phyto-C correlated significantly negatively with salinity during fall, winter, and spring. For the nutrients, phyto-C showed a significant positive correlation with SiO_3^{2-}, PO_4^{3-}, NO_2^-, and NO_3^- during fall, winter, and spring. No significant correlation was observed between phyto-C and nutrients during summer. The relationship between diatom-C and various environmental parameters was quite similar to that with phyto-C. Dinoflagellate-C correlated significantly positively with temperature in winter and significantly negatively with temperature in spring. No significant correlation was observed between dinoflagellate-C and any nutrient during all four cruises.

3.3 Dominant species and CCA analysis

The dominant phytoplankton species and their cell volume and carbon are presented in Table 3. The dominant phytoplankton species in Jiaozhou Bay were mostly diatoms during the four cruises.

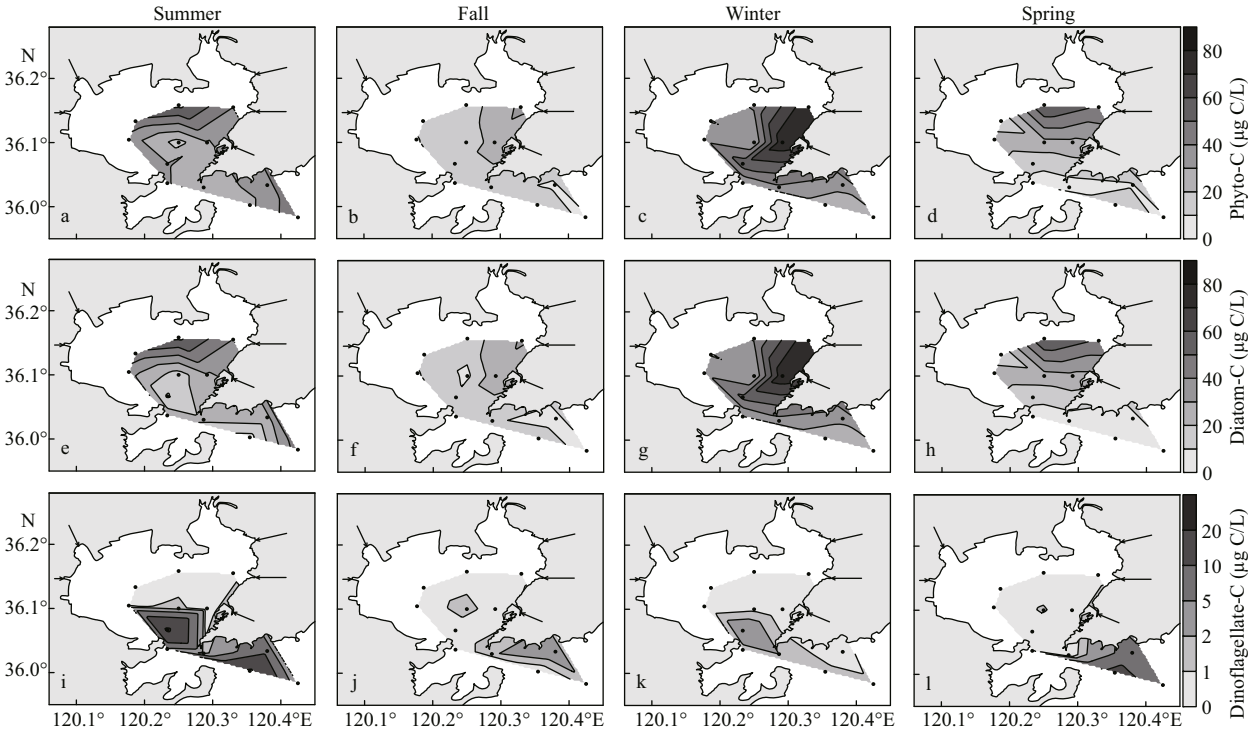

Fig.3 Distribution of phyto-C (a–d), diatom-C (e–h), and dinoflagellate-C (i–l) in the study area during four cruises

Table 2 Pearson correlation analysis (*R* values) between the phyto-C (with the dominant group: diatom and dinoflagellate) (μg C/L) and environmental parameters during four cruises in Jiaozhou Bay

Cruise		*T*	*S*	SiO_3^{2-}	PO_4^{3-}	NO_2^-	NO_3^-	NH_4^+
Summer	Phyto-C	0.108	-0.140	0.356	0.330	0.321	0.347	0.248
	Diatom-C	0.240	-0.037	0.443	0.432	0.415	0.431	0.327
	Dinoflagellate-C	-0.330	-0.141	-0.367	-0.383	-0.362	-0.357	-0.294
Fall	Phyto-C	-0.289	-0.774**	0.702*	0.753**	0.613*	0.735**	0.730**
	Diatom-C	-0.299	-0.724**	0.663*	0.743**	0.610*	0.704*	0.699*
	Dinoflagellate-C	0.206	0.080	-0.102	-0.348	-0.283	-0.174	-0.170
Winter	Phyto-C	-0.437	-0.763**	0.864**	0.824**	0.864**	0.857**	0.843**
	Diatom-C	-0.471	-0.784**	0.881**	0.847**	0.882**	0.876**	0.858**
	Dinoflagellate-C	0.666*	0.508	-0.437	-0.553	-0.451	-0.469	-0.418
Spring	Phyto-C	0.544	-0.827**	0.598*	0.611*	0.793**	0.827**	0.509
	Diatom-C	0.641*	-0.835**	0.623*	0.594*	0.805**	0.862**	0.524
	Dinoflagellate-C	-0.669*	0.394	-0.369	-0.188	-0.397	-0.515	-0.286

T: temperature; *S*: salinity. *$P<0.05$ (2-tailed); **$P<0.01$ (2-tailed).

Chaetoceros curvisetus and *Skeletonema* sp. were dominant throughout the year. For dinoflagellates, only *Ceratium fusus* in summer and *Gyrodinium spirale* and *Scrippsiella trochoidea* in spring were found to be dominant. The cell volume of the different species varied greatly. The smallest dominant species was *Skeletonema* sp., with cell volumes ranging 70–2 050 μm³ (mean ~350 μm³). The largest dominant species was *Rhizosolenia delicatula*, with cell volumes ranging 17 800–1 310 000 μm³ (mean ~164 000 μm³), which were approximately 400–500 fold that of *Skeletonema* sp. For cell carbon, *Rhizosolenia delicatula* cell carbon was about ~100 fold that of *Skeletonema* sp. cell carbon.

The CCA biplots of the dominant species carbon biomass values and environmental parameters are presented in Fig.4. In summer, *Chaetoceros curvisetus* correlated positively with nutrient concentrations (Fig.4a). *Skeletonema* sp. and *Chaetoceros decipiens* correlated negatively with salinity. *Ceratium fusus*

Table 3 Cell volume (min–max, and mean) and carbon per cell of top 5 dominant species during each cruise using the equations from Menden-Deuer and Lessard (2000)

Season	Dominant species	*n*	Volume min–max (μm³)	Volume mean (μm³)	Cell carbon (pg C/cell)
Summer	*Chaetoceros curvisetus*	30	570–8 800	3 670	224
	Chaetoceros decipiens	30	246–46 100	8 700	451
	Skeletonema sp.	35	82–1 740	349	33
	Eucampia zoodiacus	30	840–32 400	9 450	482
	Ceratium fusus	20	6 380–275 000	24 800	2 890
Fall	*Skeletonema* sp.	30	110–1 590	310	30
	Chaetoceros curvisetus	30	520–7 200	3 400	211
	Thalassiosira pacifica	30	3 150–42 500	10 500	526
	Paralia sulcata	30	1 310–59 000	6 850	372
	Eucampia zoodiacus	30	790–28 500	8 750	453
Winter	*Skeletonema* sp.	35	70–1 530	350	33
	Thalassiosira pacifica	30	2 980–48 500	9 800	497
	Rhizosolenia delicatula	30	17 800–1 310 000	164 000	4 882
	Meuniera membranacea	20	13 900–148 000	28 500	1 181
	Ditylum sol	20	17 000–195 000	57 800	2 096
Spring	*Skeletonema* sp.	30	80–2 050	420	39
	Thalassiosira angstii	30	3 450–21 500	9 310	477
	Gyrodinium spirale	20	3 420–105 000	24 900	2 901
	Chaetoceros curvisetus	30	350–11 500	2 940	187
	Scrippsiella trochoidea	30	750–17 100	4 580	592

n: number of cells measured for cell volume determination.

correlated positively with temperature. In fall, *Skeletonema* sp., *Thalassiosira pacifica*, and *Eucampia zoodiacus* correlated positively with nutrient concentrations, and *Paralia sulcata* showed no correlation with any environmental parameter (Fig.4b). In winter, *Skeletonema* sp. and *Thalassiosira pacifica* correlated positively with nutrient concentrations (Fig.4c). *Ditylum sol* correlated positively with temperature and salinity. *Meuniera membranacea* and *Rhizosolenia delicatula* showed no correlation with any environmental parameter. In spring, *Thalassiosira angstii* correlated positively with nutrient concentrations, and *Gyrodinium spirale* and *Scrippsiella trochoidea* correlated positively with salinity (Fig.4d). *Chaetoceros curvisetus* and *Skeletonema* sp. showed no correlation with any environmental parameter.

3.4 C:Chl *a* and growth rates of the phytoplankton cells

The C:Chl *a* of the phytoplankton cells during the four cruises are shown in Fig.5. In summer, the C:Chl *a* values varied from 22.84 to 52.90 (mean 38.87), and the highest value appeared at station D3, while the lowest value appeared at station A3. C:Chl *a* increased from north to south in the study area (Fig.5a). In fall, the C:Chl *a* values varied from 15.74 to 47.73 (mean 28.83), the highest value appeared at station D6, and the lowest value appeared at station C1. Generally, high C:Chl *a* values appeared in the outer bay, except for station B2 (Fig.5b). In winter, the C:Chl *a* values varied from 24.29 to 61.45 (mean 34.22), the highest value appeared at station D8, and the lowest value appeared at station D6 (Fig.5c). In spring, the C:Chl *a* values varied from 11.50 to 43.97 (mean 24.70), the highest value appeared at station D6, and the lowest value appeared at station A5. High C:Chl *a* values appeared in the outer bay (Fig.5d).

Phytoplankton growth rates in the bay ranged from 0.56 to 1.96/d; peaked in summer (mean±SD= 1.79±0.13/d), and then in fall (mean±SD=1.24±0.09/d), spring (mean±SD=1.17±0.25/d), and winter (mean± SD=0.77±0.09/d) were the lowest. Phytoplankton growth rates were significantly positively correlated with temperature and negatively correlated with salinity (Fig.6a & b). Significant positive correlation was also observed between phytoplankton growth rates and silicate concentrations (Fig.6c).

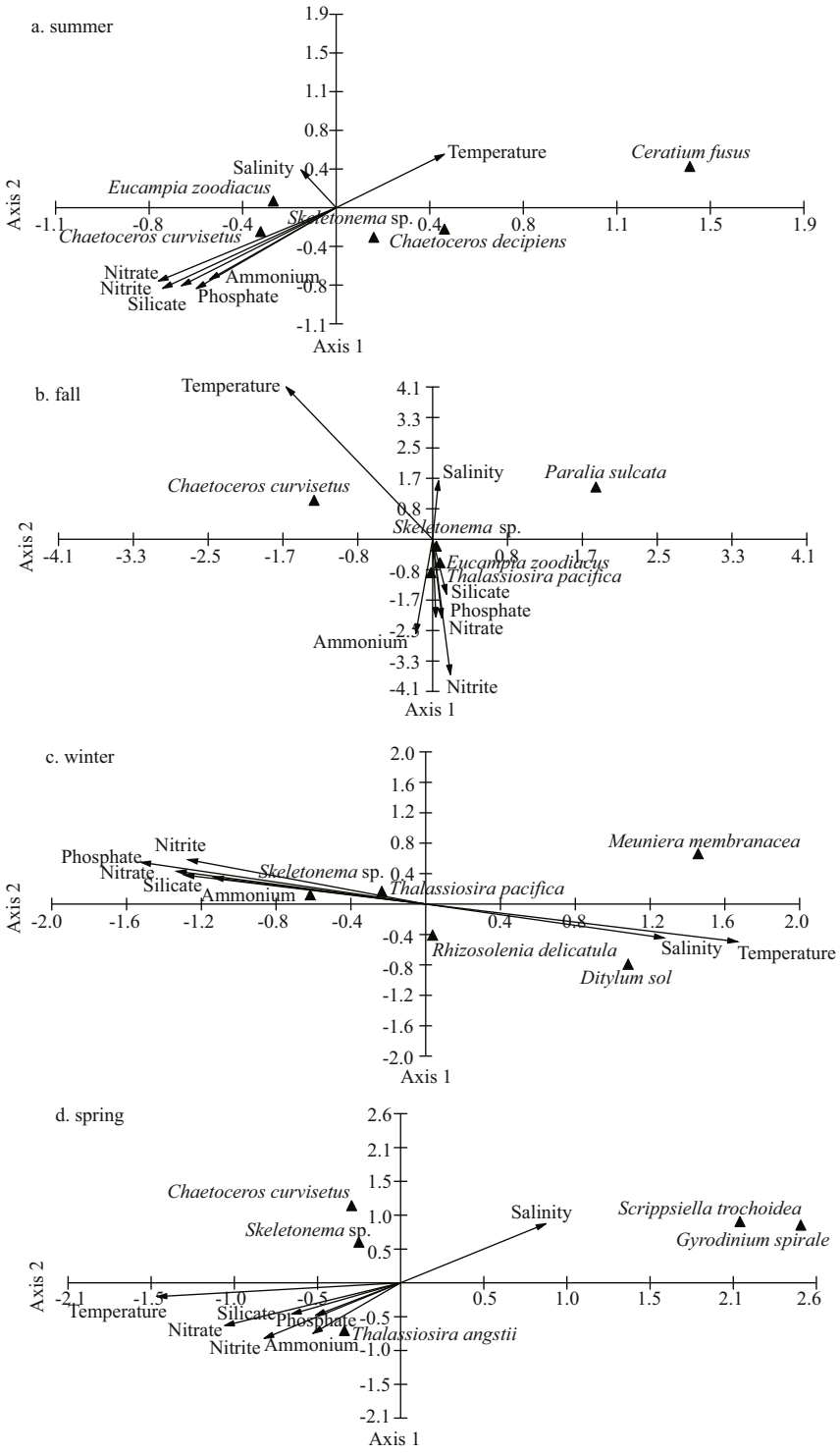

Fig.4 CCA of the dominant phytoplankton species and environmental parameters during four cruises in the bay

4 DISCUSSION

4.1 Phyto-C and its regulating factors in the Jiaozhou Bay

Accurate determination of phyto-C in natural communities has long been recognized as essential to understanding marine ecosystems and their environmental dependencies (Graff et al., 2012). Several automated and semi-automated methods for phytoplankton cell biovolume estimation have been introduced in recent years, mainly including flow cytometry and combined systems (Jakobsen and

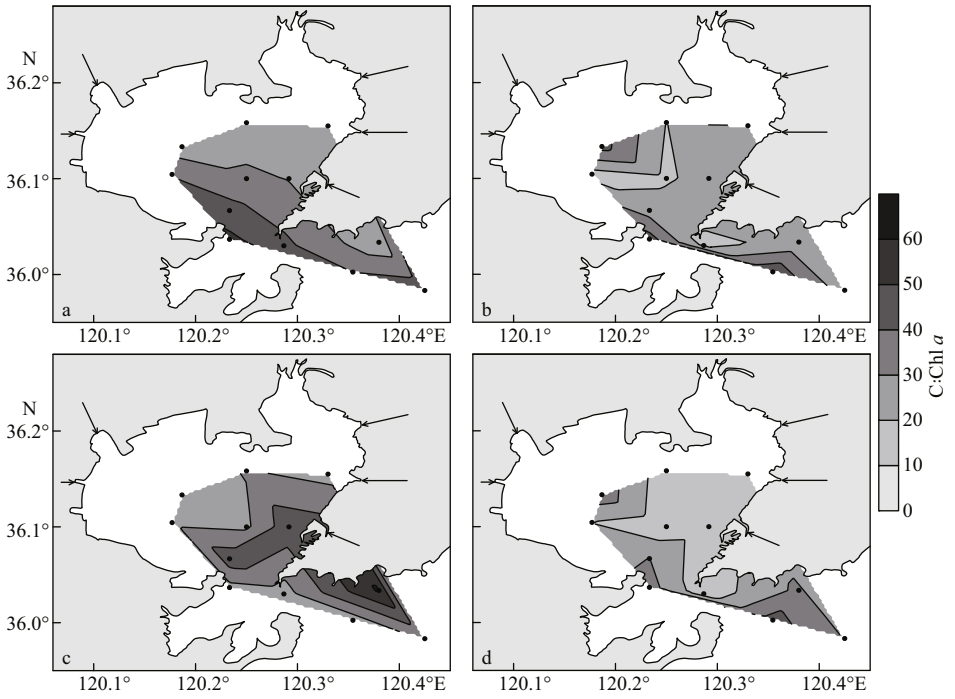

Fig.5 C:Chl *a* of phytoplankton cells during four cruises in the study area

a. summer; b. fall; c. winter; d. spring.

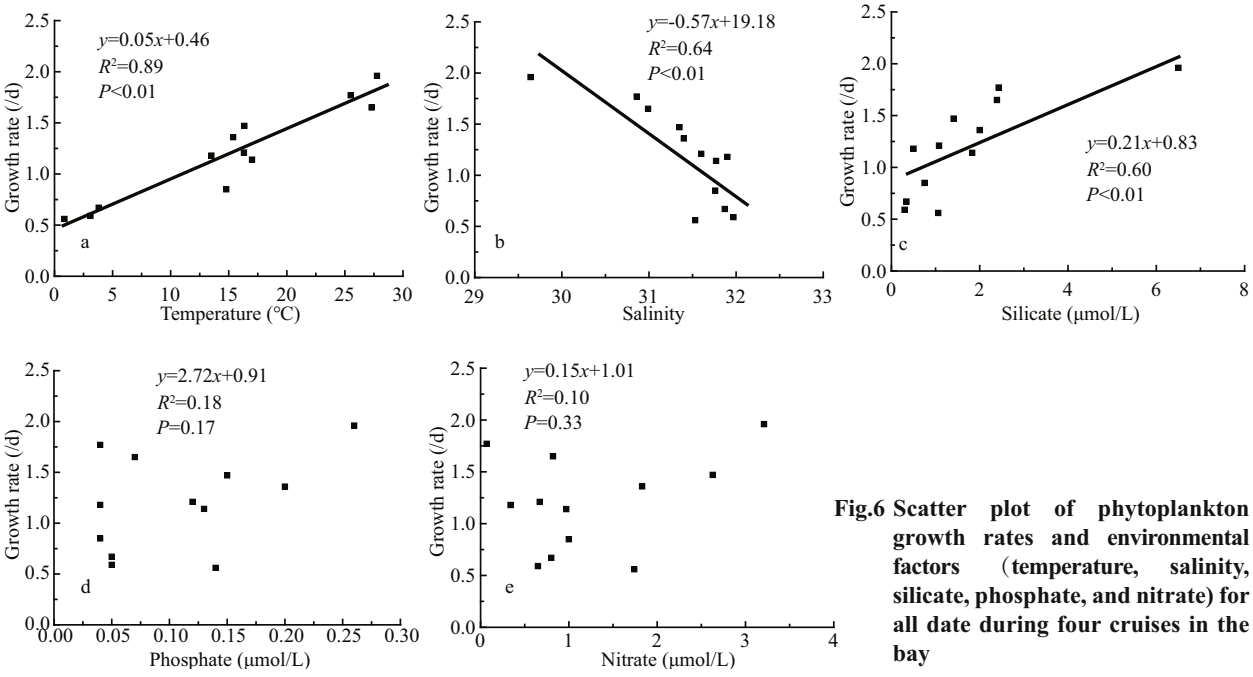

Fig.6 Scatter plot of phytoplankton growth rates and environmental factors (temperature, salinity, silicate, phosphate, and nitrate) for all date during four cruises in the bay

Carstensen, 2011; Spaulding et al., 2012; Yang et al., 2017), and this might lead to their increased use in the future. Automated methods have been proved successful in experiments with unialgal cultures or with easily discernible species in the laboratory (Hillebrand et al., 1999). However, in addition to requiring expensive equipment, taxonomic resolution with flow cytometry does not allow the distinction of species that is often necessary for marine ecological studies, which would constrain their application in some situations. At present, light microscopy is still the most commonly used method for determining phytoplankton cell biovolumes with the highest degree of accuracy (taxonomically and geometrically) (Jakobsen and Markager, 2016; Crawford et al., 2018; Ara et al., 2019).

Table 4 Phyto-C in different coastal seas around the world ocean

Location	Season	Depth (m)	Phyto-C (μg C/L)	Reference
Coastal East China Sea	Summer	Surface	142.8	Chang et al., 2003a
The Hauraki Gulf and adjacent shelf of north-eastern New Zealand	Spring	0–110 m	<10 to 400	Chang et al., 2003b
Crozet Basin	Winter	Surface	10–84	Kopczyńska and Fiala, 2003
Apalachicola Bay, Florida	Whole year	Surface	18–1 985	Putland and Iverson, 2007
Coastal waters off Cape Esan, Japan	Whole year	0–200	<10 to >300	Shinada et al., 2008
Sagami Bay	Whole year	0–50	0–316	Ara et al., 2019
Jiaozhou Bay	Whole year	Surface	5.05–78.52	This study

Phyto-C ranged from 5.05 to 78.52 μg C/L in Jiaozhou Bay, falling in the range reported in other coastal seas (Table 4). Comparing with other studies in coastal seas, the highest phyto-C value in this study seems somewhat low (Table 4). Chang et al. (2003b) studied phyto-C in the East China Sea, and found that phyto-C was 142.8 μg C/L in the coastal station, where a diatom bloom formed. In their study, the combined concentrations of nitrate and nitrite were >8 μmol/L at the coastal station, and Chl-*a* concentration exceeded 7.9 μg/L. Shinada et al. (2008) studied phyto-C in coastal waters off Cape Esan, Japan, and found that phyto-C varied from <10 to >300 μg C/L. In their study, phyto-C was lower than 100 μg C/L during the most time of the year, and high phyto-C value (>100 μg C/L) only appeard during spring diatom blooms period. Ara et al. (2019) found that phyto-C varied from 0 to 316 μg C/L (mean=17.50 μg C/L) in the Sagami Bay, and the high phyto-C value was mainly attributed to spring phytoplankton blooms with Chl *a* being as high as 14.25 μg/L. In this study, both nutrients and Chl-*a* levels (Table 1) indicated that none phytoplankton bloom occurred during the four cruises. If excluding the high phyto-C values during phytoplankton blooms period in studies of Chang et al. (2003b), Shinada et al. (2008) and Ara et al. (2019), the range of phyto-C in this study should be similar with those studies mentioned above.

Diatom-C was predominant during all four cruises, accounting for over 75% of the total phyto-C. This was consistent with the results of several other studies. Marañón et al. (2000) studied the distributions of phytoplankton biomass in the Atlantic Ocean, and found that diatoms were the dominant group, and dinoflagellates contributed less than 4% to total phyto-C. Chang et al. (2003b) found that in the coastal East China Sea, diatoms were the dominant group, and dinoflagellates contributed only 3.5% to total phyto-C. Chang et al. (2003a) studied the phytoplankton biomass in the Hauraki Gulf and adjacent shelf of northeastern New Zealand, and found that diatoms accounted for 70% to 95% of the total phyto-C. Previous studies on phytoplankton community structure based on cell counting in Jiaozhou Bay also revealed that diatoms dominated phytoplankton community structure throughout the year (Sun et al., 2011a; Guo et al., 2019).

As phytoplankton is an important component of biogeochemical cycling in the ocean, the contribution of phyto-C to total POC is an important input for biogeochemical models (Arteaga et al., 2016). In this study, phyto-C/POC ranged from 17.47% to 66.36% (mean±SD=38.16%±13.17%) in the bay. Arteaga et al. (2016) used models to study the contribution of phyto-C to the total POC pool in the global ocean and found that phytoplankton account for 30%–70% of the total POC in most of the low-latitude ocean (between 40°N and 40°S). Therefore, the mean phyto-C/POC in this study fell within the range of their model results. Pico-phytoplankton cells were not counted due to the difficulty in observing them under the microscope in this study; therefore, the phyto-C/POC was likely underestimated here. Sun and Sun (2012) found that pico-phytoplankton accounted for less than 5% of the total Chl *a* in Jiaozhou Bay, so its contribution to the POC pool should not be significant here. It should be noted that the conversion of cell volume to cell carbon also imposes a source of variation. The carbon-to-volume relationship derived by Menden-Deuer and Lessard (2000) was used to estimate phyto-C from phytoplankton cell biovolume in this study. Their analysis is based on laboratory cultures that may not naturally mirror phytoplankton assemblages. However, as we used the same conversion factor as that in Menden-Deuer and Lessard (2000) throughout the study, the spatiotemporal distribution pattern of phyto-C should not have been influenced.

In this study, phyto-C was always higher inside the bay than outside the bay (*t*-test, $P<0.05$) (Fig.3a–d)

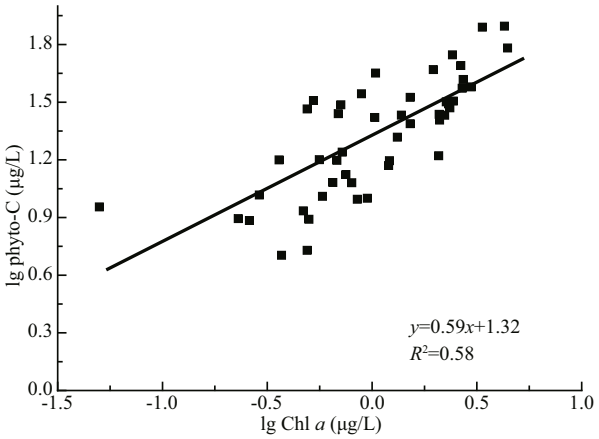

Fig.7 Lg-lg relationship between Chl *a* and phyto-C of all data points in the bay

and showed a significant positive correlation with nutrients during fall, winter, and spring (Table 2). This was consistent with previous studies on the phytoplankton community in the bay (Yang et al., 2014; Shi et al., 2015; Guo et al., 2019). Diatom-C correlated significantly positively with nutrients, while no significant correlation was observed between dinoflagellate-C and any nutrient (Table 2). Dinoflagellate-C was high in the southern part of the study area, where nutrient levels were low, which was quite different from diatom-C levels (Fig.3). Shi et al. (2015) studied the relationship between the phytoplankton community structure and environmental parameters in the bay and found similar results. This discrepancy was mostly due to the different survival strategies of diatoms and dinoflagellates. As a totally autotrophic phytoplankton group, diatoms can easily become dominant when nutrients are sufficient in the environment (Zhou et al., 2017). In this study, the distribution pattern of diatom-C was quite similar to that of nutrients (Figs.2 & 3), and high diatom-C values always appeared in the nutrient-sufficient areas (Fig.3e–h). CCA also revealed that diatom-dominant species tended to correlate positively with nutrients (Fig.4). However, diatoms are easily affected when nutrients are not sufficient in the environment (Xiao et al., 2018). In contrast to diatoms, most dinoflagellates species are mixotrophic, which would provide them with sufficient nutrients when nutrients concentrations were low in the environment (Jeong et al., 2010). Therefore, dinoflagellates possess a survival advantage over diatoms in low nutrient environments, and this advantage results in dinoflagellates having different distribution patterns than diatoms.

4.2 C:Chl *a* values in Jiaozhou Bay and their regulating factors

In marine plankton ecology, Chl-*a* concentration is one of the most frequently determined variables. Chl *a* estimates are usually determined in contexts where conversion to phytoplankton cellular carbon is desirable, e.g., for phytoplankton growth rate calculations or for food web process calculations (Arteaga et al., 2016). In these cases, a value for the ratio between phyto-C and Chl *a* is necessary, and C:Chl *a* is therefore a widely used conversion factor in aquatic studies (Jakobsen and Markager, 2016). As concentrations of pigments in phytoplankton are influenced by factors such as light and nutrients, a wide range of C:Chl *a* values are reported in the literature across laboratory and field studies, from 6 to 333 (Geider, 1987; Cloern et al., 1995; Sathyendranath et al., 2009). C:Chl *a* values of phytoplankton cells varied from 11.50 to 61.45 (mean 31.66) in this study, which was similar to those in other coastal seas (Chang et al., 2003b; Jakobsen and Markager, 2016; Ara et al., 2019), but lower than those in several oligotrophic open oceans (Wang et al., 2009; Li et al., 2010). Several studies have found a nonlinear relationship between phyto-C and Chl *a* in the field (Legendre and Michaud, 1999; Sathyendranath et al., 2009; Jakobsen and Markager, 2016):

$$\log C = \log A + \beta \times \log \text{Chl } a, \quad (4)$$

where C is phyto-C, $\log A$ is the intercept and β is the slope of the regression. The phyto-C vs. Chl *a* scatter plots of all data points in this study are shown in Fig.7. The slope (β) was 0.59, indicating that there is an overall decrease in the C:Chl *a* value with increasing Chl-*a* concentrations in Jiaozhou Bay.

In this study, high C:Chl *a* values always appeared in the outer bay (Fig.5). This was similar to the distribution pattern of transparency (Fig.2i–l) but opposite to the distribution pattern of the nitrate concentration (Fig.2m–p). Transparency was higher in the outer bay than in the inner bay (*t*-test, $P<0.05$), while nitrate concentration was lower in the outer bay than in the inner bay (*t*-test, $P<0.05$). Therefore, the variability in C:Chl *a* reveals that C:Chl *a* tends to be high under high transparency and low nutrient conditions and low during low transparency and high nutrient conditions in the bay. The controlled laboratory studies found that phytoplankton cells increase their Chl-*a* content under low light to maximize light absorption (Falkowski and Owens, 1980), which would decrease the C:Chl *a* values.

Therefore, the light condition was better in the outer bay than in the inner bay due to the high transparency, leading to higher C:Chl *a* values there. Nutrients can also affect C:Chl *a* of phytoplankton with increasing C:Chl *a* values under nutrient limitation (Geider, 1987). The process of carbon fixation in phytoplankton cells continues under a low nutrient environment, whereas the synthesis of nitrogen and cell division are restricted, causing carbon accumulation in phytoplankton cells in a low nutrient environment (Zonneveld, 1998). Furthermore, the high C:Chl *a* values in the outer bay should also be related to the high dinoflagellate-C there (Fig.3i–l). It has been reported that in comparison to other phytoplankton groups, especially diatoms, dinoflagellates have higher C:Chl-*a* values (Geider, 1987). Therefore, phytoplankton community structure should also have an impact on the spatial variation in C:Chl *a* in the bay.

4.3 Phytoplankton growth rates and their regulating factors in the bay

Quantifying phytoplankton growth rates is important to understanding many marine processes in the ocean, and growth rates govern productivity, carbon transformations within the food web, nutrient utilization and export to depths (Regaudie-de-Gioux et al., 2015). Previous studies on phytoplankton growth rates in different areas of oceans revealed that minimal growth rates ((0.1–0.2)/d) were found in oligotrophic seas, while maximal growth rates ((1.0–2.0)/d) were observed in coastal seas (Regaudie-de-Gioux et al., 2015). Tan (2009) estimated phytoplankton growth rates with the dilution method in Jiaozhou Bay and found that the values ranged from 0.38/d to 2.21/d. In this study, phytoplankton growth rates ranged from 0.56/d to 1.96/d, which were within the range of reported values. It should be noted that the primary productivity and Chl *a* were derived from total phytoplankton cells in the Eq.2, while phyto-C was derived from microscopic phytoplankton cells (not including pico-phytoplankton), therefore, phytoplankton growth rates in this study should be somewhat overestimated.

Phytoplankton growth rates were highest in summer (mean±SD=(1.79±0.13)/d), followed by those in fall (mean±SD=(1.24±0.09)/d) and spring (mean±SD=(1.17±0.25)/d), and the lowest occurred in winter (mean±SD=(0.77±0.09)/d) in the bay. A significant positive correlation was observed between growth rates and temperature in this study (Fig.6a). Several studies have reported the effect of temperature on phytoplankton growth rates in the sea (Boyd et al., 2013; Sherman et al., 2015), and the influence of temperature on growth rates exists due to the control temperature exerts on metabolic processes inside phytoplankton cells (Eppley, 1972). A commonly used function that describes the relationship between temperature and phytoplankton growth rate is the Q_{10} model,

$$g=g_0\times Q_{10}^{(T-T_0)/10}, \quad (5)$$

where g_0 is a reference growth rate (/d) at the reference temperature T_0=303.15 K (30 °C) (Eppley, 1972; Sherman et al., 2015). In this study, the temperature was highest in summer and lowest in winter, and the difference in the mean temperature values was approximately 25 °C between these two seasons (Table 1). If assuming a Q_{10} of 1.47 (Sherman et al., 2015), then a 25-°C temperature difference would lead to a 2.6-fold growth rate difference, which is consistent with the phytoplankton growth rates in summer (mean 1.79/d) and winter (mean 0.77/d) in this study.

In addition to temperature, phytoplankton growth rates were also found to be positively correlated with silicate concentrations (Fig.6c), which indicated that the silicate concentration in the bay should be the most important nutrient in determining phytoplankton growth. Most of the dominant phytoplankton species in the bay during the four cruises were diatoms (Table 3), and CCA revealed that diatom-dominant species tended to correlate positively with silicate concentrations (Fig.4). High silicate concentrations stimulate diatom growth, which induces high growth rates of the whole phytoplankton community. Several other studies also found a similar relationship between phytoplankton growth rates and nutrients. Örnólfsdóttir et al. (2004) found that natural phytoplankton communities showed a growth-rate increase response to enhanced nutrient concentrations in Galveston Bay. Stel'makh et al. (2009) found that phytoplankton growth rates and silicate and nitrate concentrations were correlated in the coastal waters of Bulgaria. Pinckney et al. (2001) measured the growth rates of phytoplankton in the Neuse River estuary with and without nutrient amendments and found that the growth rates were obviously higher when nutrients were added. In Jiaozhou Bay, several previous studies have also revealed that silicate concentrations could significantly affect phytoplankton growth (Yang et al., 2006; Yao et al., 2007). Therefore, phytoplankton growth was affected

by silicate concentration in Jiaozhou Bay.

It should be noted that phytoplankton growth rates are dictated by the abiotic controls like temperatures, light, and nutrient concentrations (Cloern et al., 1995), and the combined effects of these factors determine phytoplankton growth rates ultimately. In this study, the results of Fig.6 should be considered with caution. High temperature was an important determining factor for the high phytoplankton growth rates in summer (Fig.6a). As nutrients concentrations were also highest in summer (Table 1), high nutrients levels should also be responsible for high phytoplankton growth rates in summer. A significant negative correlation was observed between phytoplankton growth rates and salinity (Fig.6b), but it did not suggest that high salinity would inhibit phytoplankton growth here. Judging from the salinity and nutrients distribution patterns in the bay (Fig.2), the negative correlation between phytoplankton growth rates and salinity was most probably an indirect outcome of the positive correlation between phytoplankton growth rates and nutrients.

5 CONCLUSION

We studied the carbon biomass and C:Chl *a* of phytoplankton based on water samples in Jiaozhou Bay, and phytoplankton growth rates were also estimated. Phyto-C ranged from 5.05 to 78.52 μg C/L in the bay, falling within the range reported in other coastal seas. Diatom-C was predominant, accounting for over 75% of the total phyto-C during all four cruises, and diatom-C showed a significant positive correlation with nutrients. No significant correlation was observed between dinoflagellate-C and any nutrient during the four cruises. This discrepancy is mostly due to the different survival strategies of diatoms and dinoflagellates (autotrophic vs. mixotrophic). The C:Chl *a* values of phytoplankton cells varied from 11.50 to 61.45 in this study, which were similar to the values in other coastal seas and lower than those in several oligotrophic open oceans. A significant log-log relationship was found between phyto-C and Chl *a* in the bay: $\log C = 0.59 \times \log \text{Chl } a + 1.32$, where C is phyto-C, and this equation provides a reference for phytoplankton carbon calculations based on Chl *a* in subsequent studies in the bay. Phytoplankton growth rates ranged from 0.56/d to 1.96/d, falling within the range of previously reported values in the bay. Temperature and silicate levels were found to have an impact on phytoplankton growth rates in the bay.

6 DATA AVAILABILITY STATEMENT

Data are available on request from the authors.

7 ACKNOWLEDGMENT

We thank the crew and captain of the R/V *Chuangxin* for the logistic support during the cruise. Temperature, salinity, and transparency data were provided by the Jiaozhou Bay Marine Ecosystem Research Station.

References

Ara K, Fukuyama S, Okutsu T, Nagasaka S, Shiomoto A. 2019. Seasonal variability in phytoplankton carbon biomass and primary production, and their contribution to particulate carbon in the neritic area of Sagami Bay, Japan. *Plankton and Benthos Research*, **14**(4): 224-250.

Arteaga L, Pahlow M, Oschlies A. 2016. Modeled Chl:C ratio and derived estimates of phytoplankton carbon biomass and its contribution to total particulate organic carbon in the global surface ocean. *Global Biogeochemical Cycles*, **30**(12): 1 791-1 810.

Boyd P W, Rynearson T A, Armstrong E A, Fu F X, Hayashi K, Hu Z X, Hutchins D A, Kudela R M, Litchman E, Mulholland M R, Passow U, Strzepek R F, Whittaker K A, Yu E, Thomas M K. 2013. Marine phytoplankton temperature versus growth responses from polar to tropical waters-outcome of a scientific community-wide study. *PLoS One*, **8**(5): e63091.

Chang F H, Zeldis J, Gall M, Hall J. 2003a. Seasonal and spatial variation of phytoplankton assemblages, biomass and cell size from spring to summer across the north-eastern New Zealand continental shelf. *Journal of Plankton Research*, **25**(7): 737-758.

Chang J, Shiah F K, Gong G C, Chiang K P. 2003b. Cross-shelf variation in carbon-to-chlorophyll *a* ratios in the East China Sea, summer 1998. *Deep Sea Research Part II*: *Topical Studies in Oceanography*, **50**(6-7): 1 237-1 247.

Cloern J E, Grenz C, Vidergar-Lucas L. 1995. An empirical model of the phytoplankton chlorophyll: carbon ratio-the conversion factor between productivity and growth rate. *Limnology and Oceanography*, **40**(7): 1 313-1 321.

Crawford D W, Cefarelli A O, Wrohan I A, Wyatt S N, Varela D E. 2018. Spatial patterns in abundance, taxonomic composition and carbon biomass of nano- and microphytoplankton in Subarctic and Arctic Seas. *Progress in Oceanography*, **162**: 132-159.

Eppley R W. 1972. Temperature and phytoplankton growth in the sea. *Fishery Bulletin*, **70**(4): 1 063-1 085.

Falkowski P G, Owens T G. 1980. Light—shade adaptation two strategies in marine phytoplankton. *Plant Physiology*, **66**(4): 592-595.

Friedland K D, Stock C, Drinkwater K F, Link J S, Leaf R T, Shank B V, Rose J M, Pilskaln C H, Fogarty M J. 2012.

Pathways between primary production and fisheries yields of large marine ecosystems. *PLoS One*, **7**(1): e28945.

Fu M Z, Wang Z L, Li Y, Li R X, Sun P, Wei X H, Lin X Z, Guo J S. 2009. Phytoplankton biomass size structure and its regulation in the Southern Yellow Sea (China): seasonal variability. *Continental Shelf Research*, **29**(18): 2 178-2 194.

Geider R J. 1987. Light and temperature dependence of the carbon to chlorophyll *a* ratio in microalgae and cyanobacteria: implications for physiology and growth of phytoplankton. *New Phytologist*, **106**(1): 1-34.

Gong G C, Chen Y L L, Liu K K. 1996. Chemical hydrography and chlorophyll *a* distribution in the East China Sea in summer: implications in nutrient dynamics. *Continental Shelf Research*, **16**(12): 1 561-1 590.

Graff J R, Milligan A J, Behrenfeld M J. 2012. The measurement of phytoplankton biomass using flow-cytometric sorting and elemental analysis of carbon. *Limnology and Oceanography*: *Methods*, **10**(11): 910-920.

Graff J R, Westberry T K, Milligan A J, Brown M B, Dall'Olmo G, van Dongen-Vogels V, Reifel K M, Behrenfeld M J. 2015. Analytical phytoplankton carbon measurements spanning diverse ecosystems. *Deep Sea Research Part I*: *Oceanographic Research Papers*, **102**: 16-25.

Guo S J, Feng Y Y, Wang L, Dai M H, Liu Z L, Bai Y, Sun J. 2014. Seasonal variation in the phytoplankton community of a continental-shelf sea: the East China Sea. *Marine Ecology Progress Series*, **516**: 103-126.

Guo S J, Zhu M L, Zhao Z X, Liang J H, Zhao Y F, Du J, Sun X X. 2019. Spatial-temporal variation of phytoplankton community structure in Jiaozhou Bay, China. *Journal of Oceanology and Limnology*, **37**(5): 1 611-1 624.

Harrison P J, Zingone A, Mickelson M J, Lehtinen S, Ramaiah N, Kraberg A C, Sun J, McQuatters-Gollop A, Jakobsen H H. 2015. Cell volumes of marine phytoplankton from globally distributed coastal data sets. *Estuarine*, *Coastal and Shelf Science*, **162**: 130-142.

Hillebrand H, Dürselen C D, Kirschtel D, Pollingher U, Zohary T. 1999. Biovolume calculation for pelagic and benthic microalgae. *Journal of Phycology*, **35**(2): 403-424.

Jakobsen H H, Carstensen J. 2011. FlowCAM: sizing cells and understanding the impact of size distributions on biovolume of planktonic community structure. *Aquatic Microbial Ecology*, **65**(1): 75-87.

Jakobsen H H, Markager S. 2016. Carbon-to-chlorophyll ratio for phytoplankton in temperate coastal waters: seasonal patterns and relationship to nutrients. *Limnology and Oceanography*, **61**(5): 1 853-1 868.

Jeong H J, Yoo Y D, Kim J S, Seong K A, Kang N S, Kim T H. 2010. Growth, feeding and ecological roles of the mixotrophic and heterotrophic dinoflagellates in marine planktonic food webs. *Ocean Science Journal*, **45**(2): 65-91.

Kopczyńska E E, Fiala M. 2003. Surface phytoplankton composition and carbon biomass distribution in the Crozet Basin during austral summer of 1999: variability across frontal zones. *Polar Biology*, **27**(1): 17-28.

Kruskopf M, Flynn K J. 2006. Chlorophyll content and fluorescence responses cannot be used to gauge reliably phytoplankton biomass, nutrient status or growth rate. *New Phytologist*, **169**(3): 525-536.

Legendre L, Michaud J. 1999. Chlorophyll *a* to estimate the particulate organic carbon available as food to large zooplankton in the euphotic zone of oceans. *Journal of Plankton Research*, **21**(11): 2 067-2 083.

Li Q P, Franks P J S, Landry M R, Goericke R, Taylor A G. 2010. Modeling phytoplankton growth rates and chlorophyll to carbon ratios in California coastal and pelagic ecosystems. *Journal of Geophysical Research*: *Biogeosciences*, **115**(G4): G04003.

Liu D Y, Sun J, Qian S B. 2002. Study on the phytoplankton in Jiaozhou Bay II: influence of the environmental factors to phytoplankton community. *Journal of Ocean University of Qingdao*, **32**(3): 415-421. (in Chinese with English abstract)

Liu X, Huang B Q, Huang Q, Wang L, Ni X B, Tang Q S, Sun S, Wei H, Liu S M, Li C L, Sun J. 2015. Seasonal phytoplankton response to physical processes in the southern Yellow Sea. *Journal of Sea Research*, **95**: 45-55.

Lü S G, Wang X C, Han B P. 2009. A field study on the conversion ratio of phytoplankton biomass carbon to chlorophyll-*a* in Jiaozhou Bay, China. *Chinese Journal of Oceanology and Limnology volume*, **27**(4): 793-805.

Marañón E, Holligan P M, Varela M, Mouriño B, Bale A J. 2000. Basin-scale variability of phytoplankton biomass, production and growth in the Atlantic Ocean. *Deep Sea Research Part I*: *Oceanographic Research Papers*, **47**(5): 825-857.

Menden-Deuer S, Lessard E J. 2000. Carbon to volume relationships for dinoflagellates, diatoms, and other protist plankton. *Limnology and Oceanography*, **45**(3): 569-579.

Örnólfsdóttir E B, Lumsden S E, Pinckney J L. 2004. Phytoplankton community growth-rate response to nutrient pulses in a shallow turbid estuary, Galveston Bay, Texas. *Journal of Plankton Research*, **26**(3): 325-339.

Pinckney J L, Richardson T L, Millie D F, Paerl H W. 2001. Application of photopigment biomarkers for quantifying microalgal community composition and in situ growth rates. *Organic Geochemistry*, **32**(4): 585-595.

Putland J N, Iverson R L. 2007. Phytoplankton biomass in a subtropical estuary: distribution, size composition, and carbon: chlorophyll ratios. *Estuaries and Coasts*, **30**(5): 878-885.

Regaudie-de-Gioux A, Sal S, López-Urrutia Á. 2015. Poor correlation between phytoplankton community growth rates and nutrient concentration in the sea. *Biogeosciences*, **12**(6): 1 915-1 923.

Sathyendranath S, Stuart V, Nair A, Oka K, Nakane T, Bouman H, Forget M H, Maass H, Platt T. 2009. Carbon-to-chlorophyll ratio and growth rate of phytoplankton in the sea. *Marine Ecology Progress Series*, **383**: 73-84.

Sherman E, Moore J K, Primeau F, Tanouye D. 2015. Temperature influence on phytoplankton community growth rates. *Global Biogeochemical Cycles*, **30**(4): 550-

559.

Shi X Y, Wang L S, Yang S M. 2015. Phytoplankton community of Jiaozhou Bay in winter 2010. *Oceanologia et Limnologia Sinica*, **46**(2): 357-364. (in Chinese with English abstract)

Shinada A, Ban S, Ikeda T. 2008. Seasonal changes in the planktonic food web off Cape Esan, southwestern Hokkaido, Japan. *Plankton and Benthos Research* (*Japan*), **3**(1): 18-26.

Smith Jr W O, Nelson D M, Mathot S. 1999. Phytoplankton growth rates in the Ross Sea, Antarctica, determined by independent methods: temporal variations. *Journal of Plankton Research*, **21**(8): 1 519-1 536.

Spaulding S A, Jewson D H, Bixby R J, Nelson H, McKnight D M. 2012. Automated measurement of diatom size. *Limnology and Oceanography*: *Methods*, **10**(11): 882-890.

Stel'makh L V, Babich I I, Tugrul S, Moncheva S, Stefanova K. 2009. Phytoplankton growth rate and zooplankton grazing in the western part of the Black Sea in the autumn period. *Oceanology*, **49**(1): 83-92.

Sun J, Liu D Y, Qian S B. 1999. Study on phytoplankton biomass I. Phytoplankton measurement biomass from cell volume or plasma volume. *Acta Oceanologica Sinica*, **21**(2): 75-85. (in Chinese with English abstract)

Sun J, Liu D Y, Qian S B. 2000. Estimating biomass of phytoplankton in the Jiaozhou Bay I. Phytoplankton biomass estimated from cell volume and plasma volume. *Acta Oceanologica Sinica*, **19**(2): 97-110.

Sun J, Liu D Y. 2003. Geometric models for calculating cell biovolume and surface area for phytoplankton. *Journal of Plankton Research*, **25**(11): 1 331-1 346.

Sun X X, Sun S, Wu Y L, Zhang Y S, Zheng S. 2011a. Long-term changes of phytoplankton community structure in the Jiaozhou Bay. *Oceanologia et Limnologia Sinica*, **42**(5): 639-646. (in Chinese with English abstract)

Sun X X, Sun S, Zhang Y S, Zhang F. 2011b. Long-term changes of chlorophyll-*a* concentration and primary productivity in the Jiaozhou Bay. *Oceanologia et Limnologia Sinica*, **42**(5): 654-661. (in Chinese with English abstract)

Sun X X, Sun S. 2012. Phytoplankton size structure and its temporal and spatial changes in Jiaozhou Bay. *Oceanologia et Limnologia Sinica*, **43**(3): 411-418. (in Chinese with English abstract)

Tan S J. 2009. Preliminary Studies on Cascade Grazing of Mesozooplankton on Phytoplankton and Microzooplankton Community in the Jiaozhou Bay. Ocean University of China, Qingdao. (in Chinese)

Utermöhl H. 1958. Zur vervollkommnung der quantitativen phytoplankton-methodik. *SIL Communications*, *1953-1996*, **9**(1): 1-38.

Wang X J, Borgne R L, Murtugudde R, Busalacchi A J, Behrenfeld M. 2009. Spatial and temporal variability of the phytoplankton carbon to chlorophyll ratio in the equatorial Pacific: a basin-scale modeling study. *Journal of Geophysical Research*, **114**(C7): C07008.

Wu Y L, Sun S, Zhang Y S. 2005. Long-term change of environment and it's influence on phytoplankton community structure in Jiaozhou Bay. *Oceanologia et Limnologia Sinica*, **36**(6): 487-498. (in Chinese with English abstract)

Xiao W P, Liu X, Irwin A J, Laws E A, Wang L, Chen B Z, Zeng Y, Huang B Q. 2018. Warming and eutrophication combine to restructure diatoms and dinoflagellates. *Water Research*, **128**: 206-216.

Yang D F, Gao Z H, Sun P Y, Zhao B, Li M. 2006. Spatial and temporal variations of the primary production limited by nutrient silicon and water temperature in the Jiaozhou Bay. *Advances in Marine Science*, **24**(2): 203-212. (in Chinese with English abstract)

Yang S M, Wang L S, Shi X Y. 2014. Phytoplankton community of the Jiaozhou Bay in spring 2009. *Oceanologia et Limnologia Sinica*, **45**(6): 1 234-1 240. (in Chinese with English abstract)

Yang Y, Sun X X, Zhu M L, Luo X, Zheng S. 2017. Estimating the carbon biomass of marine net phytoplankton from abundance based on samples from China seas. *Marine and Freshwater Research*, **68**(1): 106-115.

Yao Y, Zheng S Q, Shen Z L. 2007. Study on the mechanism of eutrophication in the Jiaozhou Bay. *Marine Science Bulletin*, **26**(4): 91-98. (in Chinese with English abstract)

Zhou W H, Yin K D, Long A M, Huang H, Huang L M, Zhu D D. 2012. Spatial-temporal variability of total and size-fractionated phytoplankton biomass in the Yangtze River Estuary and adjacent East China Sea coastal waters, China. *Aquatic Ecosystem Health & Management*, **15**(2): 200-209.

Zhou Y P, Zhang Y M, Li F F, Tan L J, Wang J T. 2017. Nutrients structure changes impact the competition and succession between diatom and dinoflagellate in the East China Sea. *Science of the Total Environment*, **574**: 499-508.

Zonneveld C. 1998. A cell-based model for the chlorophyll *a* to carbon ratio in phytoplankton. *Ecological Modelling*, **113**(1-3): 55-70.